13th World Conference on Earthquake Engineering
Vancouver, B.C., Canada
August 1-6, 2004
Paper No. 369

SEISMIC COEFFICIENTS FOR PSEUDOSTATIC SLOPE ANALYSIS

Cristiano MELO[1] and Sunil SHARMA[2]

SUMMARY

Pseudostatic analysis is one of the simplest approaches used in earthquake engineering to analyze the seismic response of soil embankments and slopes. However, the choice of seismic coefficients used in the analysis can be arbitrary and generally lacks rationale. To investigate this, a parametric study was performed on a soil embankment of varied geometric characteristics and soil properties subjected to three different strong ground motions obtained during the 1994 Northridge earthquake. The dynamic response of the embankment model was used to calculate seismic coefficient time histories for critical failure surfaces generated through conventional limit equilibrium analysis. FLAC, a two-dimensional explicit finite difference program developed by the Itasca Consulting Group for engineering mechanics computations, was used for the dynamic analysis. The soil behavior was modeled by the Mohr-Coulomb constitutive relationship. Once the seismic coefficient time histories were obtained, a procedure was used to compute weighted average seismic coefficients for each of the time histories. The weighted average seismic coefficients obtained in this fashion were analyzed for possible correlations with the parameters used in the study. The results obtained should provide a more rational approach for selecting seismic coefficients for pseudostatic analysis.

1.0 INTRODUCTION

Limit equilibrium analysis has traditionally been used to assess the stability of slopes. This procedure consists of analyzing the cross section of the potential slide mass, called the failure surface (refer to line ab in Figure 1), as either a circular or non-circular surface. The area enclosed between the slope face and the failure surface, known as the failure mass, is subdivided into a series of slices which are then analyzed for equilibrium by several computational methods. In earthquake prone areas, horizontal and vertical pseudostatic (seismic) coefficients, k_h and k_v, respectively, are used to compute the horizontal and vertical forces caused by a potential earthquake, as shown in Figure 1. These forces are in turn added to the overall equilibrium computation for the individual slices composing the failure surface. Studies based on Newmark's displacement-type analysis (Newmark [1]) and field observations indicate that the pseudostatic method can be useful in evaluating the performance of embankments constructed of soils that do not lose significant strength during earthquakes. Such soils include clays, clayey soils, dry or moist cohesionless soils, and dense cohesionless soils (Seed [2]).

[1]Senior Staff Engineer, Kleinfelder, Inc., Pleasanton, USA. Email: cmelo@kleinfelder.com
[2] Professor, University of Idaho, Moscow, USA. Email: ssharma@uidaho.edu

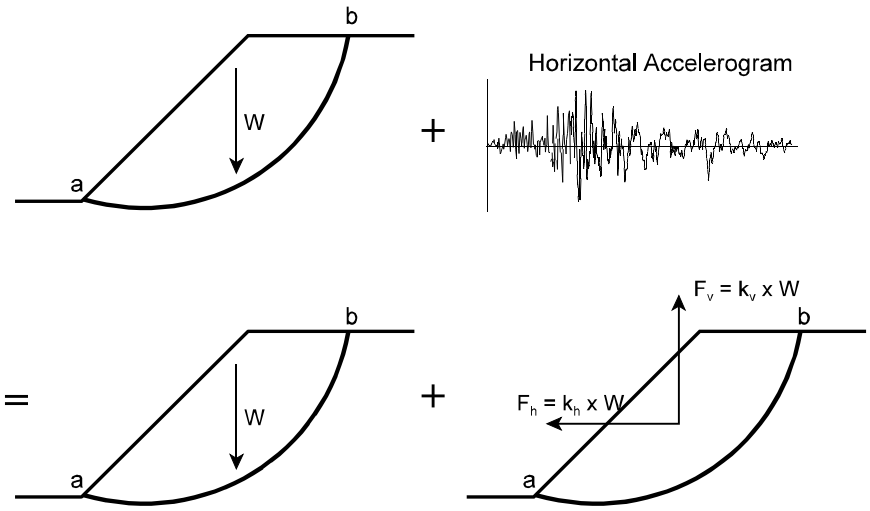

Figure 1 Pseudostatic analysis approach.

Selection of an appropriate seismic coefficient is the most important, and difficult, aspect of a pseudostatic stability analysis. In theory, the seismic coefficient values should depend on some measure of the amplitude of the inertial force induced in the slope by the dynamic forces generated during an earthquake. Because soil slopes are not rigid and the peak acceleration generated during an earthquake last for only a very short period of time, seismic coefficients used in practice generally correspond to acceleration values well below the predicted peak accelerations (Kramer [3]). However, the choice of coefficients used in the slope stability analysis is very subjective and lacks a clear rationale. Table 1 below shows horizontal seismic coefficient values that have been recommended for design.

Table 1 – Recommended Horizontal Seismic Coefficients

Horizontal Seismic Coefficient, k_h	Description	
0.05 - 0.15	In the United States	
0.12 - 0.25	In Japan	
0.1	"severe" earthquakes	Terzaghi [4]
0.2	"violent, destructive" earthquakes	
0.5	"catastrophic" earthquakes	
0.1 - 0.2	Seed [2], FOS $\geq$ 1.15	
0.10	Major Earthquake, FOS > 1.0	Corps of Engineers [5]
0.15	Great Earthquake, FOS > 1.0	
½ to ⅓ of PHA	Marcuson [6], FOS >1.0	
½ of PHA	Hynes-Griffin [7], FOS > 1.0	
FOS = Factor of Safety. PHA = Peak Horizontal Acceleration, in g's.		

As shown in Table 1, there are no specific rules for selection of an appropriate seismic coefficient for design. However, the different selection criteria suggest that the seismic coefficient should be based on the anticipated level of acceleration within the failure mass and should correspond to some fraction of the anticipated peak acceleration (Kramer [3]).

Due to the limitations in the selection process of seismic coefficients used in design, a parametric study was performed on a soil embankment of varied geometric characteristics and soil properties subjected to three different strong ground motions obtained during the 1994 Northridge earthquake. The two-dimensional explicit finite difference program FLAC was used to perform the static and dynamic analyses of the embankment. Based on the seismic response obtained from FLAC, seismic coefficients were computed for the different embankment slopes analyzed. It is hoped that the results of the study will allow practitioners to choose seismic coefficients based on the specific geometry and properties of a slope, as well as the characteristics of a specific design earthquake.

2.0 NUMERICAL ANALYSIS OF SLOPES

The finite element method has been used extensively to analyze stresses in a variety of man-made and natural slopes, especially embankment slopes where the desired stresses are often located along a curved failure surface through the interior of the embankment. The accuracy of a finite element analysis depends on the type of element used, fineness of mesh, mesh layout, the geometry of the problem, and the constitutive model used to simulate the stress-strain behavior of the soils. The different discretization schemes used in finite element analysis of slopes during the last three decades show great variability in the size and shape of the elements used. For an embankment of height H, element heights range from H/4 to H/25, with H/10 being the most popular value. The most commonly used element is either a three or four node element, but in the last decade, eight and nine node elements have become more common. The element aspect ratios (height/width) have usually been close to one, but ranging from 1/3 to 3 (Ashford [8]).

Several computer programs that are based on either the finite element or the finite difference method have been used to perform seismic analysis of soil embankments. Some examples of programs used to perform seismic analysis of soil embankment slopes include QUAD-4, FLUSH, and FLAC. The set of algebraic equations solved by the finite difference method is identical to that solved with the finite element method for a given number of element shape functions. However, in the finite difference method, the set of algebraic equations is solved using dynamic relaxation, an explicit, time-marching procedure in which the full dynamic equations of motion are integrated step by step. Static solutions are computed by including damping terms that gradually remove kinematic energy from the system (Dawson [9]).

Version 3.3 of FLAC, which stands for Fast Lagrangian Analysis of Continua, was used in the parametric study discussed here (Itasca Consulting Group [10]). FLAC is a time domain, two-dimensional explicit finite difference program used for engineering mechanics computations. This program is primarily intended for geotechnical engineering applications and simulates the behavior of models/structures composed of soil, rock, or other materials that may undergo plastic flow when their yield limits are reached. Materials are represented by quadrilateral elements, which form a mesh or grid that is shaped as the object to be modeled. Elements and grid points are numbered in a row-and-column fashion rather than in a sequential manner. The program uses two dimensional arrays (I,J) and (i,j) to define the elements and nodes, respectively, within its discrete mesh. An uppercase "I" and a lowercase "i" specify the location of an element and a node, respectively, columnwise, from left to right, starting at column one, while an uppercase "J" and a lowercase "j" specify the location of an element and a node, respectively, rowwise, from bottom to top, starting at row one. The grid elements within the mesh behave according to a prescribed linear or non-linear stress/strain behavior in response to the applied forces or boundary restraints. The material can yield and flow, and the mesh can deform and move with the material that is represented. FLAC has ten built-in material models. For dynamic analysis, user-specified acceleration, velocity, or stress waves can be input directly to the model either as an

exterior boundary condition or as an interior excitation to the model. The program contains absorbing and free-field boundary conditions to simulate the effect of an infinite elastic medium surrounding the model.

3.0 ANALYSIS OF SLOPES USING FLAC

The model used in the study consisted of a homogeneous earth embankment of varying heights, H, and slope grades, H:V, overlying a 5-meter thick homogeneous soil foundation layer, as shown in Figure 2. The foundation layer was underlain by bedrock. The soil behavior was modeled in FLAC as a linear, perfectly plastic material with a Mohr-Coulomb yield condition and an associated flow rule. No tension cut-off was specified, and the Mohr-Coulomb yield condition was assumed to be valid in the tensile normal stress domain, which meant that the failure envelope intersected the normal axis at -c/tanϕ. Small-strain mode was used for the static portion of the analyses (i.e., the coordinates of the grid points composing the finite difference mesh were not updated according to the computed nodal displacements). Large-strain mode was used for the dynamic portion of the study, such that grid coordinates were updated based on nodal displacements. No water table was specified for the study and pore water pressures were assumed to be zero.

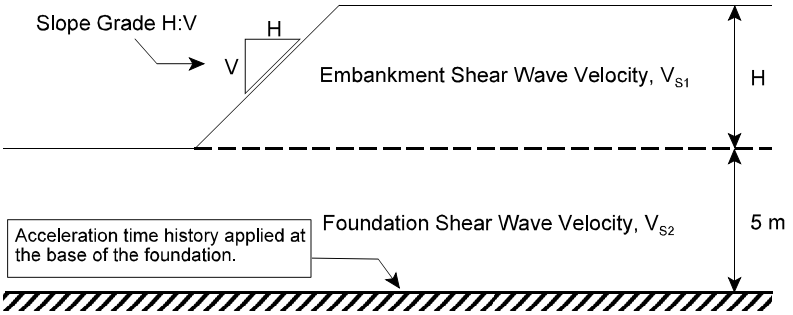

Figure 2 Embankment model used in the study.

The different embankments were first analyzed for static conditions to allow for the computation of static stresses along their respective critical failure surfaces once static equilibrium was reached. Then, the embankments were subjected to three different earthquake acceleration time histories to permit the computation of the dynamic stresses along their respective critical failure surfaces. The difference in stresses for the dynamic and static conditions was then used to calculate seismic coefficient time histories. Next, a weighted average was taken of the computed seismic coefficient time histories, as discussed in Section 4.0.

3.1 Embankment Parameters

The four parameters varied throughout the study are shown in Figure 2, and included the embankment's height, H, the embankment's and its foundation's shear wave velocity, V_{S1} and V_{S2}, the embankment's slope face grade, H:V, and the input acceleration time histories. These parameters were chosen because they appear to play an important role in influencing the dynamic response of soil embankments. For instance, embankments tend to achieve resonant conditions whenever their natural frequency matches the predominant frequency of the input ground motion. In addition, the natural frequency of an embankment, f_n, as shown by Equation 1, is influenced by the embankment's height and its shear wave velocity.

$$f_n = \frac{V_S}{4H} \qquad (1)$$

Table 2 shows the variation in embankment slope grade, slope height, and shear wave velocity, for the study. The soil strength parameters used (unit weight, γ, internal angle of friction, ϕ, and cohesion, c) remained constant throughout the parametric study because they did not appear to influence the resulting seismic coefficients as significantly as the selected parameters. However, the elastic shear modulus, G, and the elastic bulk modulus, K, did vary because they were dependent on the shear wave velocity. Table 3 presents the embankment and foundation soil properties common to all the analyses performed.

Table 2 - Parameters for the Soil Embankment and Foundation

Slope Grade	Slope Height, H	Shear Wave Velocities, V_S	Elastic Shear Modulus, G	Elastic Bulk Modulus, K
	(m)	(m/s)	(kPa)	(kPa)
1H:1V	5	$V_E = 800$ $V_F = 400$	$G_E = 1.174 \times 10^6$ $G_F = 2.936 \times 10^5$	$K_E = 3.523 \times 10^6$ $K_F = 8.807 \times 10^5$
1.5H:1V	10	$V_E = 800$ $V_F = 800$	$G_E = 1.174 \times 10^6$ $G_F = 1.174 \times 10^6$	$K_E = 3.523 \times 10^6$ $K_F = 3.523 \times 10^6$
2H:1V	15	$V_E = 400$ $V_F = 800$	$G_E = 2.936 \times 10^5$ $G_F = 1.174 \times 10^6$	$K_E = 8.807 \times 10^5$ $K_F = 3.523 \times 10^6$
Subscript E = Embankment, subscript F = Foundation.				

Table 3 - Embankment and Foundation Soil Properties Common to all Analyses

Unit Weight, γ (kN/m^3)	Internal Angle of Friction, ϕ (degrees)	Cohesion, c (kPa)	Poisson's Ratio, ν	Rayleigh Damping (%)
18.0	35.0	10.0	0.35	0.1

3.2 Input Accelerograms

The three free-field horizontal earthquake acceleration time histories used in the study were recorded during the Northridge earthquake of January 17, 1994 ($M_w = 6.7$). No scaling factors were applied to the corrected time histories. Table 4 shows the characteristics of the accelerograms used. As noted in Figure 2, the input accelerograms were applied at the base of the soil foundation, just above the bedrock layer.

Table 4 - Characteristics of the Accelerograms used in this Study

Location	Arleta - Nordhoff Avenue Fire Station	Century City - LACC North	Lake Hughes 12A
Epicentral Distance (km)	9.65	19.31	38.62
Bracketed Duration (seconds)	24.42	14.38	7.69
PHA (g's)	0.344	0.256	0.174
Predominant Period	1.187	0.598	0.281

3.3 Number of Analyses Performed

The variations in the problem studied generated 81 possible analyses (3 slopes x 3 heights x 3 shear modulus combinations x 3 acceleration time histories = 81 analyses). The 81 analyses were grouped into 9 geometries (3 slopes x 3 heights = 9), each containing 9 property combinations. Note that because the shear modulus, G, and the bulk modulus, K, are dependent on the shear wave velocities shown in Table 2, their values did not contribute to the increase in the number of analyses necessary to perform the parametric study.

3.4 Mesh Layout

The following mesh layouts were used for the 81analyses performed in this study:

1. 120 meters wide and 10 meters high.
2. 120 meters wide and 15 meters high.
3. 20 meters wide and 20 meters high.

From these three basic meshes, adjustments were made in the slope angle to simulate the nine possible slope geometries (3 slope heights x 3 slope grades = 9 geometries). All elements were one meter wide by one meter high, except those near the slope face. Figure 3 shows the mesh used for the 5-meter high embankment with a slope grade of 1H:1V. The right and left boundaries of the mesh were fixed only in the horizontal direction (this condition is represented by rollers in Figure 3), while the base was fixed in both the horizontal and vertical directions (this condition is represented by pins in Figure 3). The critical failure surface, line ab, is also shown in this figure. For clarity, a truncated mesh is shown in Figure 3, where zones labeled as "50 elements" and "950 elements" have an additional 10 columns by 5 rows and 95 columns by 10 rows of elements, respectively.

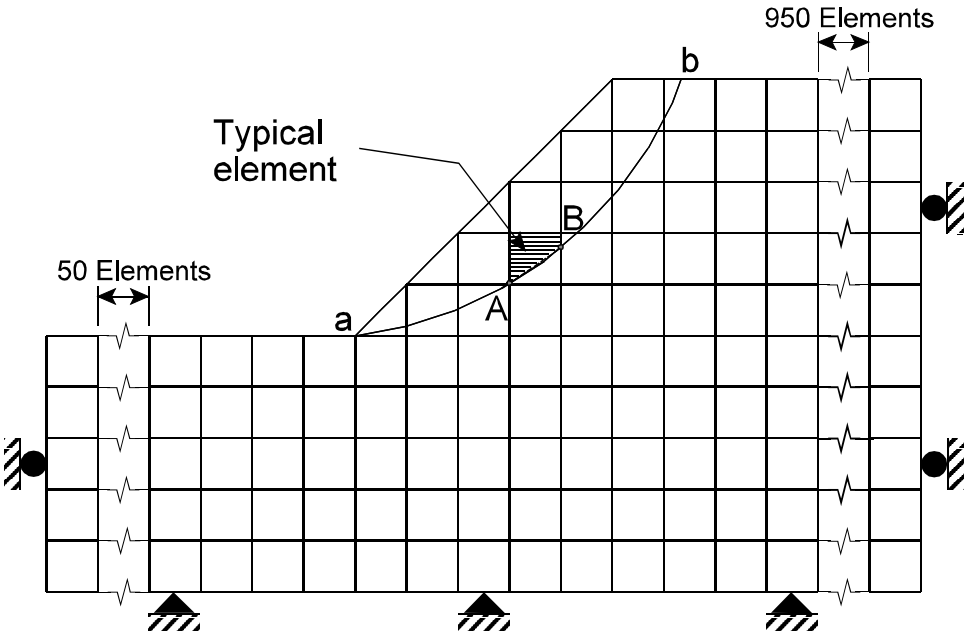

Figure 3 Discrete finite difference mesh used for the 5-meter high embankment with a slope of 1H:V.

4.0 METHODOLOGY

The first step in the study was to identify the critical failure surface for the different earth embankments analyzed. Once this task was accomplished, several discrete finite difference meshes were set up to perform the static and dynamic analyses of the earth embankments using FLAC. The seismic coefficient time histories computed in these analyses were then used to calculate average seismic coefficient values. These average values were dependent on the duration and amplitude of the individual cycles composing the seismic time histories. The following sections describe these procedures in detail.

4.1 Generation of Failure Surfaces Using XSTABL

The modified Bishop method in the slope stability program XSTABL, version 5.2, was used to identify the critical circular failure surfaces for the different slope configurations (Interactive Software Designs [11]). The search strategy for each embankment geometry involved the generation of 1,600 circular failure surfaces. The restrictions placed on the failure surface search strategy were as follows:

- The failure surface start point was located at the toe of the slope.
- The failure surface daylighted behind the crest of the embankment slope.
- The failure surface end point was located between the slope crest and a point 20 meters behind the slope crest.

These restrictions were placed in the search strategy because the critical failure surface for homogeneous soil embankments with a foundation layer are generally expected to start at the toe of the slope and to remain within the embankment layer, as demonstrated by Griffiths [12].

4.2 Failure Surface Setup in FLAC

The critical failure surface geometry generated in XSTABL was used to plot the failure surface over the discrete finite difference mesh. Then, the failure surface was divided into straight line segments every time it crossed an element boundary. At each element boundary, either the x or y coordinate was known. The unknown failure surface segment coordinates were computed using Equation 2, which defines a circle.

$$(x - x_c)^2 + (y - y_c)^2 = r^2 \qquad (2)$$

Note that x and y are the coordinates of any point along the circle, x_c and y_c are the coordinates of the center of the circle, and r is the radius of the circle. Once the coordinates for the segments were determined using Equation 2, the horizontal and the vertical components of the segments' lengths were computed.

4.3 Computation of Seismic Coefficients

As shown in Figure 1, the weight of the soil mass inside the failure surface as well as the resultant horizontal and vertical forces acting on the failure surface must be known in order to compute the horizontal and vertical seismic coefficients. The total weight of the soil mass inside the failure surface can be computed once the failure wedge geometry is known. A similar approach to that employed by Chopra [13] was used to compute the horizontal and vertical forces acting at the centroid of the failure surface. The approach consisted of first breaking the failure surface into several segments, with each segment lying inside a discrete finite element. Figure 3 shows a finite difference mesh with the failure surface simulated by several straight line segments, while Figure 4 shows a typical element found along the failure surface.

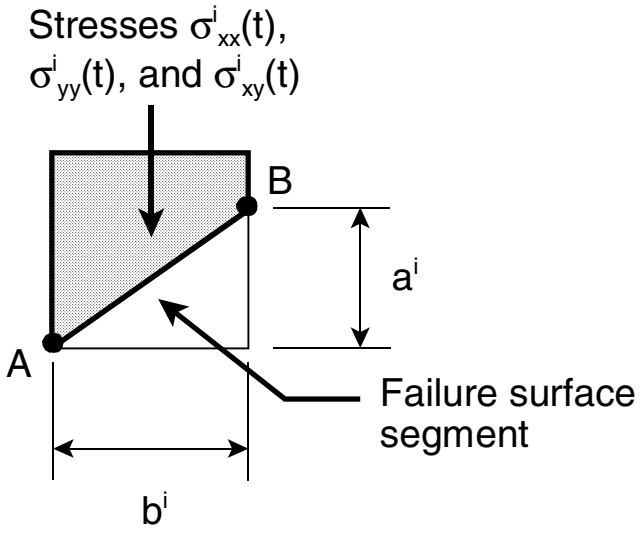

Figure 4 Typical element showing the linear approximation of the circular failure surface between segment points.

The horizontal and vertical forces acting on each segment composing the critical failure surface were computed using the stresses present in each segment at the end of the static analysis. This was accomplished using Equations 3 and 4, where b^i and a^i are the horizontal and vertical components of the segment's length (line AB in Figure 4) and σ^i_{xx}, σ^i_{yy}, and σ^i_{xy} are the horizontal, vertical, and shear stresses present in the segment. Figure 5 shows the positive stress sign convention used in FLAC (note that tension is positive) along with the positive sign convention used in the study to compute the forces acting on each segment.

$$F_h(t) = \sum_i a^i \sigma^i_{xx}(t) - b^i \sigma^i_{xy}(t) \qquad (3)$$

$$F_v(t) = -\sum_i a^i \sigma^i_{xy}(t) - b^i \sigma^i_{yy}(t) \qquad (4)$$

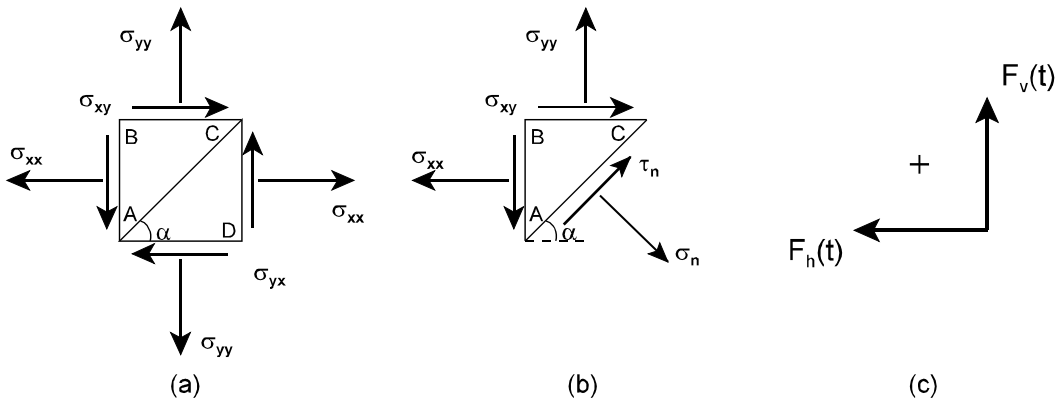

Figure 5 (a) Positive sign convention for normal and shear stresses in FLAC, (b) free body diagram of ABC as shown in (a), and (c) positive sign convention used to compute forces acting on the failure surface.

Next, the sum of the forces acting along the failure surface segments were divided by the weight of the entire failure wedge, yielding the static coefficients for the entire failure surface, as illustrated in Figure 6. The same process described above was used to compute dynamic coefficients at every timestep during the dynamic analysis. Once this was accomplished, the static coefficients recorded at the end of the static analysis were subtracted from the dynamic coefficient time history computed during the dynamic analysis. In this fashion, a time history of seismic coefficients was produced over the duration of the input ground motion, as shown in Figure 6.

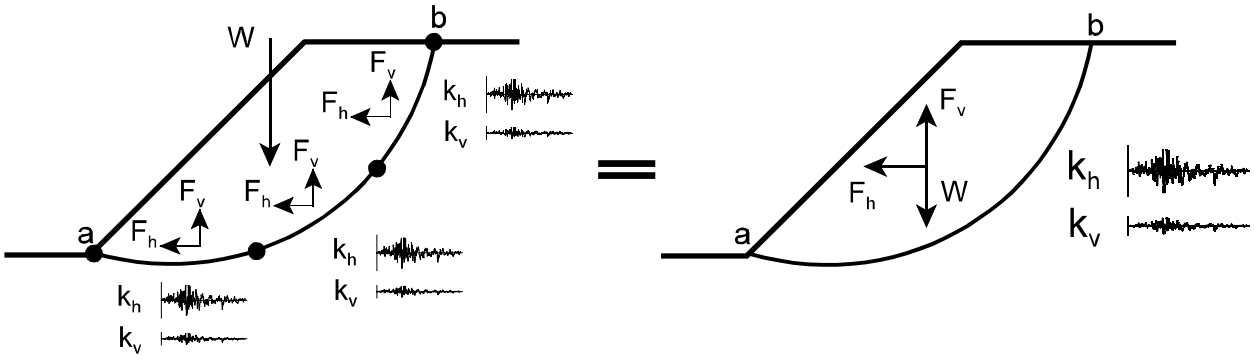

Figure 6 Methodology used in the computation of seismic coefficients.

4.4 Analysis of Seismic Coefficient Time Histories

After each dynamic FLAC analysis was completed, the computed horizontal and vertical seismic coefficient time histories were simplified (smoothed). The procedure consisted of connecting the starting and ending points of each positive or negative motion cycle to the absolute maximum value in the cycle, as shown by the doted lines connecting Figures 7(a) and 7(b). In this fashion, the erratic peaks contained in each motion cycle of Figure 7(a) were replaced by a single peak, as shown in Figure 7(b).

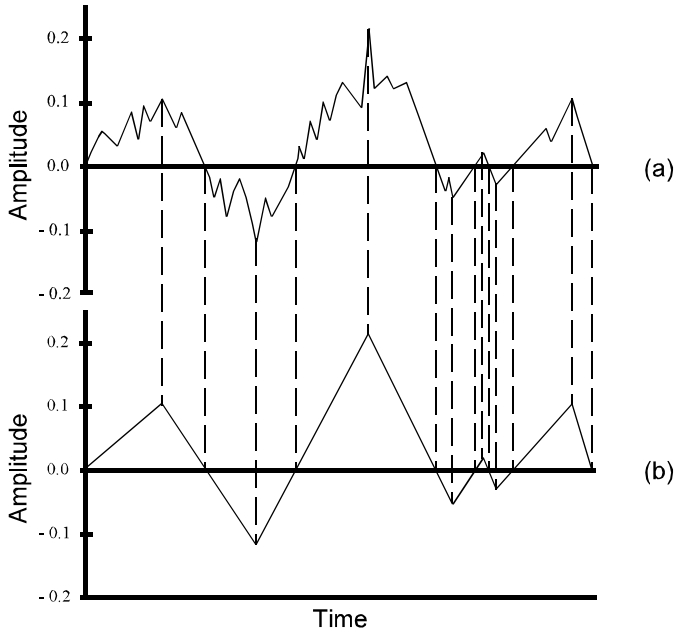

Figure 7 (a) Actual, erratic FLAC response, (b) Simplified, smoothed version of the same output. Dashed lines connect relevant, common portions of the two graphs.

Next, a weighted average was taken of the smoothed horizontal and vertical seismic coefficient time histories. The approach used the duration of each significant peak, those most likely to cause damage to the slope during an earthquake, to weigh its contribution towards an average peak value. The duration of the individual peaks was defined as the base of the triangular shaped peaks (units of time). The method reduced the contribution of short lived high peaks towards the computation of the average peak value. On the other hand, the weighted approach increased the influence of lasting low peaks towards the computation of the average peak value. The weighted average procedure consisted of three steps, as follows:

1. The significant peak coefficients were defined as those found within the first and the last cycles of the recorded time history which exceeded absolute values greater than or equal to 0.05. A significant level of 0.05 was chosen because it is the lowest seismic coefficient value recommended for design in the United States (refer to Table 1). This approach is similar to the bracketed duration proposed by Bolt [14].
2. The significant peak coefficients selected in step one were multiplied by their corresponding durations.
3. The absolute values of the weighted peak coefficients obtained in step two were summed and the result was divided by the sum of the significant durations.

The steps outlined above are summarized in Figure 8. After the weighted average procedure was applied to the seismic coefficient time history, a single average peak remained, as shown in Figure 9. The peak's amplitude increased gradually at the start of the significant duration, reached the average peak value at a time equal to half of the significant duration, and dissipated steadily to the end of the significant duration. In a similar fashion, steady stress build up and subsequent stress dissipation takes place along a soil embankment during an earthquake. Therefore, the weighted average scheme used in the study appears to represent well the actual field behavior of an earth embankment exposed to shaking motions.

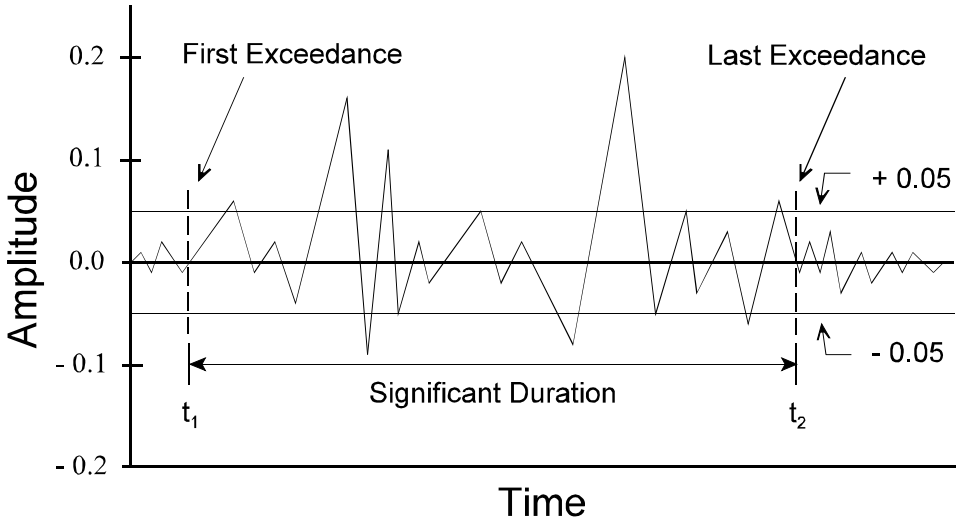

Figure 8 Weighted average scheme.

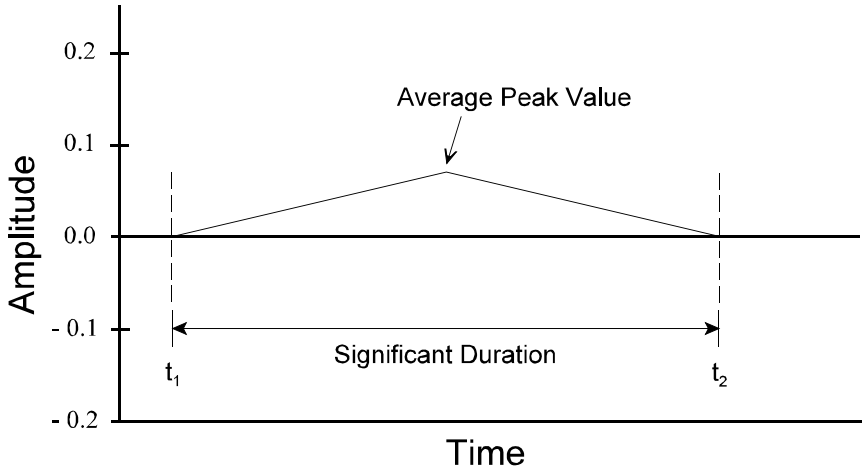

Figure 9 Equivalent single peak.

5.0 RESULTS AND DISCUSSIONS

5.1 Seismic Coefficient Results

Table 5 presents a summary of the 81 k_h and k_v time history results generated using FLAC. The computed absolute peak values of k_h (row 1, column 1) ranged from 0.172 to 0.677. These values are high in comparison to the recommended design coefficients shown in Table 1. By contrast, the weighted average of k_h (row 2, column 1) ranged from 0.054 to 0.213. These values are well within the range of recommended values presented in Table 1, and seem to validate the accuracy and appropriateness of the methodology used in the study. In addition, a mean value of 0.459 was obtained for the ratio of the weighted average of k_h to PHA. This value is, very interestingly, close to the k_h = ½ × PHA recommended by Hynes-Griffin [7] in Table 1.

Table 5 – Summary of the k_h and k_v Time Histories Generated in FLAC

Description			Range (1)	Mean (2)	Standard Deviation (3)
k_h	1	Absolute Peak value	0.172 - 0.677	0.367	0.094
	2	Weighted average	0.054 - 0.213	0.112	0.029
	3	Ratio of weighted average to PHA	0.212 - 0.897	0.459	0.156
	4	Significant Duration (seconds)	10.43 - 27.94	20.84	5.14
k_v	5	Absolute Peak value	0.002 - 0.301	0.091	0.072
	6	Weighted average	0.000 - 0.081	0.027	0.024
	7	Ratio of weighted average to PHA	0.000 - 0.431	0.167	0.079
	8	Significant Duration (seconds)	0.000 - 22.13	5.08	5.83
PHA in units of g's.					

The ratio between the mean of the peak k_h values (0.367; row 1, column 2) and the mean of the peak k_v values (0.091; row 5, column 2) was about four. In a similar fashion the ratio of the mean of the weighted average results for k_h and k_v (rows 2 and 6, column 2) was also approximately four. These ratios show that the vertical pseudostatic forces developed along the failure surface during the study contained considerably shorter amplitudes and durations when compared to the respective horizontal pseudostatic forces. For instance, only 52 of the 81 analyses performed in the study yielded weighted average values and significant durations for k_v. As such, 29 k_v time histories never exceeded the specified significant level of ± 0.05 discussed in Section 4.4. As a result, the mean of the weighted average of k_v time histories was 0.027, which was approximately half of 0.05, the minimum seismic coefficient value recommended for design in the United States (refer to Table 1).

5.2 Trends in the Results

In general, results indicate that steeper slopes generate higher seismic coefficients than flatter ones. In addition, the seismic coefficients appear to be directly proportional to the embankment height. As expected, the seismic coefficients also appear to be directly proportional to the PHA of the input ground motion. These results seem reasonable because flatter and shorter slopes would be expected to develop lower amplification of the shaking motions through their soil layers, all other properties being equal.

The shear wave velocity combinations had the strongest trend of all the parameters studied, which emphasizes the importance of the seismic properties of the embankment and foundation materials towards the response of the soil slope. Amplification, or de-amplification, of the earthquake motions propagating through an embankment depend on the frequency content of the input motions and the natural frequency of the soil embankment. Typically, the greatest amplification of the input ground motions will occur whenever the natural frequency of the embankment-foundation system is close to the predominant frequency of the input motions.

The analyses in which the embankment had a higher shear wave velocity (stiffer) than the foundation yielded the highest seismic coefficients, while the reverse was true for the analyses in which the embankment had a lower shear wave velocity (less stiff) than the foundation. This indicates that flexible soil structures placed on top of stiff foundations are more stable than stiff soil structures placed over flexible foundations. The most stable embankments (lowest seismic coefficients computed) were those having the same shear wave velocity as the foundation. In this case, without an impedance contrast between the embankment and foundation, the input motions were not amplified.

5.3 Possible Correlations

As part of the study, correlations (charts) were developed based on the geometry of soil embankments and properties, as well as characteristics of the design earthquake. Because of the small computed values of k_v, the study concentrated on analyzing the more significant k_h histories only. Three charts were proposed, with each chart assigned to one of the three slope grades used in the study (27 data points per chart). The independent axis (i.e., x-axis) was composed of the predominant frequency of the design earthquake, f_{acc}, normalized with respect to the natural frequency of the combined embankment and foundation, f_n. Equations 1 and 5 were used to compute the combined natural frequency of the embankment and the foundation (H_1 and H_2 correspond to the height of the embankment and foundation, respectively). The dependent axis (i.e., y-axis) was composed of the weighed average k_h value normalized with respect to the PHA.

$$V_{S\,(combined)} = \frac{\left(H_1 + H_2\right)}{\left(\frac{H_1}{V_{S1}} + \frac{H_2}{V_{S2}}\right)} \qquad (5)$$

The charts developed show that a linear relationship exists between the parameters used and the computed weighted average values of k_h. However, additional data would be necessary to improve the correlation. Figure 10 shows the correlation chart developed for a 1H:1V slope. If the linear fit (solid line) shown on this chart is extended to the right of the chart, unacceptably high k_h values will result (k_h/PHA > 1.0). Therefore, as the data points in the charts move to the right of the independent axis, the linear trend should increase up to a resonance condition and then drop, as depicted by the dashed lines in Figure 10. This anticipated behavior would resemble a magnification factor plot for the response of linear single degree of freedom systems (for reference, see Kramer [3]).

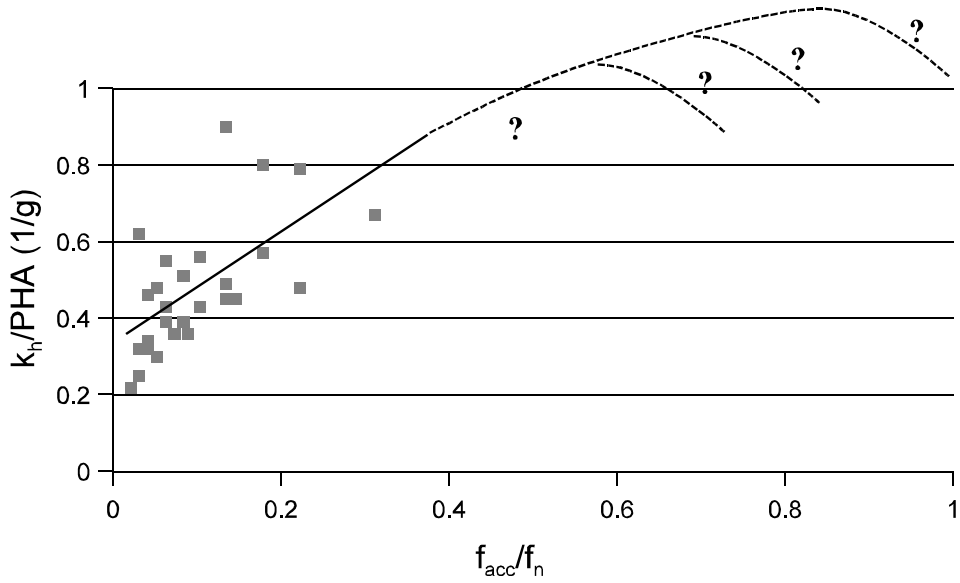

Figure 10 Possible relationship for k_h as the data points move to the right of the suggested charts developed in the study (figure based on the 1H:1V slope).

In addition to the correlations described above, another procedure based on the ratio of the computed weighted average k_h values to PHA was used in the attempt to choose suitable coefficients for design. A solver routine was used to assess the fraction of k_h/PHA that would give the lowest cumulative absolute residual for the 81 analyses performed in the study. The fraction of PHA that yielded the lowest cumulative absolute residual resulted in $k_h = 0.422 \times$ PHA. Based on this result, the k_h value of ½ PHA recommended by Hynes-Griffin [7] appears to define an upper bound in the choice of seismic coefficients for design.

6.0 SUMMARY AND CONCLUSIONS

A parametric study was performed on a soil embankment in order to assess the dependency of seismic coefficients to the geometry and properties of soil slopes, as well as the characteristics of input ground motions. An approach that accounted for the duration of the transient forces applied along the critical failure surface during different earthquakes was developed. The procedure weighted the highest computed seismic coefficient values based on the actual distribution of the energy content within the recorded time history. The approach yielded results that were representative of the overall dynamic forces developed during the earthquakes. The seismic coefficients computed in this fashion were consistent with the current state of practice.

For instance, the mean of the ratio of the weighted average of k_h to PHA was 0.459 and the best linear fit for the ratio of the weighted average of k_h to PHA was 0.422. These results suggest that perhaps k_h values ranging from 40 to 45 % of the PHA should be used in slope stability design, rather than the 50 % of the PHA proposed by Hynes-Griffin [7], whose study was subjective and relied on Newmark's [1] displacement methodology.

Because only horizontal accelerograms were used in the study, the vertical seismic coefficients computed were considerably smaller than the horizontal ones. However, as pointed out by Chopra [15] and Idriss [16], when the effects of the vertical component of ground motions are included in a seismic analysis study, larger vertical seismic coefficients are computed. These larger values, then become relevant to slope stability analysis.

Potential design charts for seismic coefficients were proposed based on the parameters varied in the study. As an added bonus to using the finite difference method in the analyses, potential design charts for horizontal displacements near the slope face were also proposed based on the parameters of interest. It is hoped that these relationships will benefit and add to the expanding database concerning the choice of seismic coefficients for design, as well as the displacements experienced along the slope face of an embankment during an earthquake.

7.0 CLOSURE

Additional details of the study discussed here are presented in the masters of science thesis issued in 2000 by Melo [17]. For instance, correlation charts developed from the seismic coefficients results obtained from FLAC as well as information on the horizontal and vertical displacement obtained from the 81 analyses performed were not presented here due to the space constraints.

As in the case of all scientific models, there are certain limitations associated with this study. The model used relied on the pseudostatic approach, which assumes that the soil embankment behaves as a rigid body, and that the accelerations developed during the earthquake are uniform throughout the embankment section and are equal at all times to the ground acceleration. However, in reality the embankment does not behave as a rigid body because the accelerations developed through the embankment will vary geometrically and temporally.

Furthermore, the study did not take into account pore pressure generation and dissipation (pore water pressures were assumed to be zero). Also, the Mohr-Coulomb soil model used to represent the soil continuum does not account for strength degradation due to cyclic loading. These two conditions are critical when analyzing soil embankments composed of liquefiable materials. Another limitation in the study involved the number of analyses performed. The 81 data points could only provide limited information concerning possible trends in the parametric study.

The study presented here could be expanded in the future to include the contribution of the vertical component of earthquake ground motions, pore pressure generation, and soil strength degradation towards the overall response of soil embankments to earthquake motions. Also, the soil foundation thickness could be varied in the new analysis.

8.0 REFERENCES

1. Newmark NM. "Effects of earthquakes on dams and embankments." Géotechnique, 1965, Vol. 15, No. 2, pp. 139-160.
2. Seed HB. "Considerations in the earthquake-resistant design of earth and rockfill dams." Géotechnique, 1979, Vol. 29, No. 3, pp. 215-263.
3. Kramer SL. "Geotechnical Earthquake Engineering." Prentice-Hall, Inc., Upper Saddle River, New Jersey 07458, 1996, pp. 434-437.
4. Terzaghi K. "Mechanisms of Landslides." Engineering Geology (Berkeley) Volume, Geological Society of America, 1950.
5. Corps of Engineers. "Slope Stability Manual EM-1110-2-1902." Washington, D. C.: Department of the Army, Office of the Chief of Engineers, 1982.
6. Marcuson WF, Franklin AG. "Seismic Design, Analysis, and Remedial Measures to Improve the Stability of Existing Earth Dams - Corps of Engineers Approach", in Seismic Design of Embankments and Caverns, T.R. Howard, Ed., New York, ASCE, 1983.
7. Hynes-Griffin ME, Franklin AG. "Rationalizing the seismic coefficient method." U.S. Army Corps of Engineers Waterways Experiment Station, Vicksburg, Mississippi, 1984, Miscellaneous Paper GL-84-13, 21 pp.
8. Ashford SA, Sitar N. "Seismic Response of Steep Natural Slopes." Earthquake Engineering Research Center, College of Engineering, University of California, Berkeley, California, May 1994, Report No. UCB/EERC-94/05.
9. Dawson EM, Roth WH, Drescher A. "Slope Stability Analysis by Strength Reduction." Géotechnique, 1999, Vol. 49, No. 6, pp. 835-840.
10. Itasca Consulting Group. "FLAC, Fast Lagrangian Analysis of Continua, Version 3.3." Itasca Consulting Group, Minneapolis, Minnesota, USA, 1996.
11. Interactive Software Designs. "XSTABL, An Integral Slope Stability Analysis Program for Personal Computers, Version 5.2." Interactive Software Designs, Moscow, Idaho, USA, 1994.
12. Griffiths DV, Lane PA. "Slope stability analysis by finite elements." Géotechnique, 1999, Vol. 49, No. 3, pp. 387-403.
13. Chopra AK. "Earthquake Response of Earth Dams." Journal of the Soil Mechanics and Foundation Division, 1967, ASCE, Vol. 93, No. SM2, Proc. Paper 5137, pp. 65-81.
14. Bolt BA. "Duration of Strong Motion," Proceedings of the 4th World Conference on Earthquake Engineering, Santiago, Chile, 1969, pp. 1304-1315.
15. Chopra AK, Clough RW. "Earthquake Response of Homogeneous Earth Dams." Soil Mechanics and Bituminous Materials Research Laboratory, University of California, Berkeley, California, November 1965, Report No. TE-65-11.
16. Idriss IM, Seed HB. "Response of Earthbanks During Earthquakes," Journal of the Soil Mechanics and Foundation Division, 1967, ASCE, 93(SM3), pp. 61-82.
17. Melo C. "Seismic Coefficients for Pseudostatic Slope Analysis." Master of science thesis, College of Graduate Studies, University of Idaho, December 2000.